

**ABSTRACT:** The passive mechanical properties of small muscle fiber bundles obtained from surgical patients with spasticity ( $n = 9$ ) and patients without neuromuscular disorders ( $n = 21$ ) were measured in order to determine the relative influence of intracellular and extracellular components. For both types of patient, tangent modulus was significantly greater in bundles compared to identical tests performed on isolated single cells ( $P < 0.05$ ). However, the relative difference between bundles and single cells was much greater in normal tissue than spastic tissue. The tangent modulus of normal bundles ( $462.5 \pm 99.6$  MPa) was 16 times greater than normal single cells ( $28.2 \pm 3.3$  MPa), whereas the tangent modulus of spastic bundles ( $111.2 \pm 35.5$  MPa) was only twice that of spastic muscle cells ( $55.0 \pm 6.6$  MPa). This relatively small influence of the extracellular matrix (ECM) in spastic muscle was even more surprising because spastic muscle cells occupied a significantly smaller fraction of the total specimen area ( $38.5 \pm 13.6\%$ ) compared to normal muscle ( $95.0 \pm 8.8\%$ ). Based on these data, normal muscle ECM is calculated to have a modulus of 8.7 GPa, and the ECM from spastic muscle of only 0.20 GPa. These data indicate that spastic muscle, although composed of cells that are stiffer compared to normal muscle, contains an ECM of inferior mechanical strength. The present findings illustrate some of the profound changes that occur in skeletal muscle secondary to spasticity. The surgical implications of these results are discussed.

*Muscle Nerve* 28: 464–471, 2003

## INFERIOR MECHANICAL PROPERTIES OF SPASTIC MUSCLE BUNDLES DUE TO HYPERTROPHIC BUT COMPROMISED EXTRACELLULAR MATRIX MATERIAL

RICHARD L. LIEBER, PhD,<sup>1</sup> EVA RUNESSON, PhD,<sup>2</sup> FREDRIK EINARSSON, MD,<sup>2</sup> JAN FRIDÉN, MD, PhD<sup>2</sup>

<sup>1</sup> Departments of Orthopaedics and Bioengineering, University of California and Veterans Administration Medical Centers, 3350 La Jolla Village Drive, San Diego, California 92161, USA

<sup>2</sup> Departments of Hand Surgery and Orthopaedics, Sahlgrenska University Hospital, Göteborg, Sweden

Accepted 10 June 2003

The primary emphasis of research on spasticity has been to characterize the static and dynamic properties of the nervous system, since this is the location of the lesion.<sup>3</sup> The structural and functional properties of skeletal muscle have received far less attention, primarily due to the invasive nature of methods required to study this tissue. In addition, the relatively large amount of tissue required for functional muscle studies limits their application in the study of human disease. Reports suggesting muscle abnormalities are found in the literature, but are based on indirect calculations of joint dynamics or static measurement of biopsy properties.<sup>17,19–21</sup>

Recently, we reported a method whereby complete mechanical and structural analyses could be performed on isolated single cell segments obtained from patients with spasticity during the course of reconstructive surgery to correct joint deformities.<sup>5</sup> Structural integrity of the cellular segment appears to be maintained with these methods as shown by the maintenance of clear laser light diffraction patterns from the myofibrillar array within the cell. This study presented evidence that the resting sarcomere length of cells from patients with spasticity was significantly shorter than in normal individuals. Furthermore, the tangent modulus of “spastic cells” (i.e., cells obtained from patients with spasticity) was found to be almost two times greater than the modulus of normal cells. We hypothesized that the increased modulus (a value that represents a normalized “stiffness”) of spastic cells might explain the subjective impression of increased muscle stiffness during intraoperative manipulation of spastic muscles. To test this hypothesis, we repeated analogous

**Abbreviations:** ANOVA, analysis of variance; ATP, adenosine triphosphate; ECM, extracellular matrix; MHC, myosin heavy chain

**Key words:** biomechanics; collagen; elasticity; extracellular matrix; sarcomere length; spasticity

**Correspondence to:** R. L. Lieber; e-mail: rlieber@ucsd.edu

© 2003 Wiley Periodicals, Inc.

mechanical studies on small muscle fiber bundles that are maintained within their native connective tissue matrix (5–20 muscle cells per bundle). This approach enables partitioning of the tissue modulus into intracellular and extracellular components. This extracellular milieu represents a dynamic component of normal muscle tissue. Indeed, disruptions of the muscle's extracellular matrix (ECM) receptors leads to dystrophic phenotypes in animal models.<sup>28</sup> Since it is not possible to test mechanically the ECM directly, comparison of properties between single cells and fiber bundles is the only way to quantify the biomechanical properties of the ECM.

The current study has revealed that, although the isolated cells of spastic muscles may be stiffer compared to normal cells, bundles from spastic muscle are actually *less* stiff compared to normal muscle fiber bundles because the ECM from spastic cells has inferior material properties. These data may have significant implications in understanding the etiology of muscle changes secondary to upper motor-neuron lesions in general, and may also provide quantitative information for surgeons regarding the structural basis of the “feel” of spastic musculature.

## METHODS

**Patient Characteristics and Biopsy Procedures.** All patients included in this study, or their parents, provided informed consent for the muscle biopsies that were obtained secondary to planned surgical procedures. All procedures were performed with full approval of the Human Ethics Committee at Göteborg University as well as the Committee on the Use of Human Subjects in Research at the University of California, San Diego and VA Medical Centers. Patients with spasticity suffered from static perinatal encephalopathy (cerebral palsy), whereas “control” patients were those undergoing surgery for non-neuromuscular disorders such as fracture repair, joint fusion, and tendon repair. As a result, the patients with spasticity were significantly younger ( $9.3 \pm 3.1$  years) than control patients ( $27.5 \pm 5.4$  years,  $P < 0.001$ ). Biopsies were obtained from a variety of different muscles depending on the surgical procedure implemented. For spastic bundles, data are reported for the biceps brachialis ( $n = 3$ ), extensor carpi radialis longus ( $n = 1$ ), flexor carpi ulnaris ( $n = 2$ ), pronator teres ( $n = 2$ ), and subscapularis ( $n = 1$ ) muscles. For normal bundles, data are reported for adductor pollicis longus ( $n = 9$ ), brachioradialis ( $n = 1$ ), extensor carpi radialis longus ( $n = 3$ ), flexor digitorum superficialis III ( $n = 5$ ), and flexor digitorum superficialis V ( $n = 3$ ).

**Sample Preparation.** Biopsies were treated in exactly the same manner as previously described.<sup>5</sup> Briefly, biopsies were excised and immediately placed in a muscle-relaxing solution composed of (mM): EGTA, 7.5; potassium propionate, 170; magnesium acetate, 2; imidazole, 5; creatine phosphate, 10; adenosine triphosphate (ATP), 4; leupeptin, 17  $\mu\text{g}/\text{ml}$ ; and E64, 4  $\mu\text{g}/\text{ml}$ , to prevent protein degradation.<sup>13,27</sup> Biopsy size was typically a cylinder with dimensions of 10–15 mm in length and 2 mm in diameter, and consisted of  $\sim 1500$  fibers, at least half of which were completely intact. Almost all biopsies (28 of 30) were stored in a solution composed of relaxing solution mixed with 50% glycerol and stored at  $-20^\circ\text{C}$ ; the remaining 2 biopsies were tested without storage. No obvious effects of storage were noted. Over a period of approximately 10 months, a total of 12 biopsies were obtained from spastic patients, and 22 biopsies were obtained from normal patients.

**Mechanical Testing Protocol.** Small bundles were dissected from biopsies while in chilled relaxing solution under  $40\times$  magnification (Leica MZ8, Heerbrugg, Switzerland) with epi-illumination (Model DCR II, Fostec, Auburn, NY) using microsurgical forceps (P-00019, S&T, Neuhausen, Switzerland), and transferred to an experimental chamber filled with relaxing solution. After transfer and prior to mounting, the bundle was transilluminated with a 7-mW He–Ne laser beam to define slack sarcomere length. The device calibration was checked at the conclusion of the experiment, and the mean absolute diffraction error for the 30 experiments reported here was  $2.24 \pm 3.83\%$  (mean  $\pm$  standard deviation). The dissected bundle segment was then secured on either side to 125- $\mu\text{m}$  titanium wires using two individual 9-0 silk suture loops that were required to prevent sample slippage. One wire was secured to an ultrasensitive (sensitivity 10 V/g) force transducer (Model 405, Aurora Scientific, Aurora, Canada) and the other was secured to a micromanipulator. Structural integrity of the bundles treated in this way was excellent as evidenced by the clear striation patterns (Fig. 1) and diffraction patterns (see below). To enable comparison to previously published data,<sup>5</sup> the testing protocol was designed to measure the bundle's elastic properties apart from any velocity-dependent properties.<sup>6</sup> As such, the fiber bundle was elongated in steps with stress-relaxation permitted between steps so that velocity of stretch was irrelevant. Bundle length and diameter were calculated from a digital photo image (Model

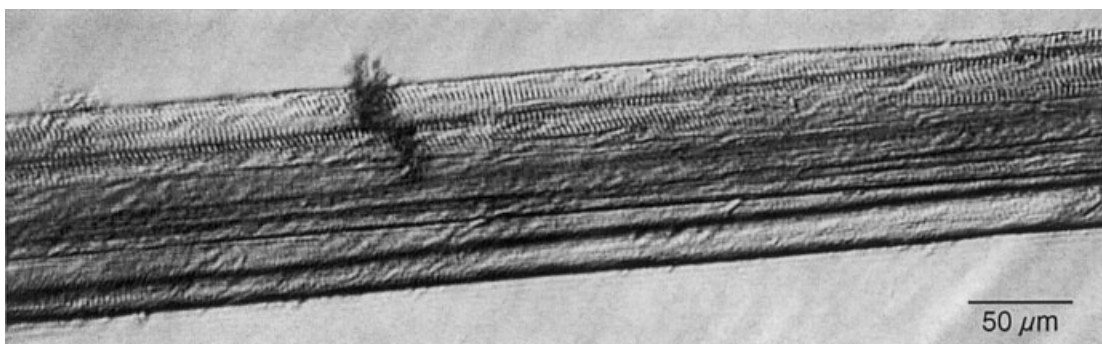


**FIGURE 1.** Central portion of a skeletal muscle bundle secured to titanium wires (not shown) for mechanical testing. Clear striation pattern visible in several fibers provides evidence of muscle cell structural integrity.

DC300, Leica). Bundle diameter was converted to bundle area assuming a circular cross-section.

Bundles were then lengthened in 250- $\mu\text{m}$  increments after which stress-relaxation was permitted for 2 min, and sarcomere length, tension, and bundle diameter (after each 500- $\mu\text{m}$  increment) were again recorded. This amount of time has been shown to permit tension to fall to within  $\sim 10\%$  of baseline values<sup>5</sup> so that tension levels reflected elastic as opposed to viscoelastic mechanical properties. Bundles were elongated until mechanical failure of any of the fibers within the bundle occurred, which resulted in a precipitous loss of tension. The sarcomere length and force recorded just prior to the lengthening that resulted in failure were defined as peak sarcomere length and used to calculate ultimate stress, respectively. Fiber bundle tangent modulus was calculated as the slope of the fiber's stress-strain curve according to the following equation:

$$E_f = \frac{\Delta\sigma_f}{\Delta\epsilon_f} = \frac{(\sigma_{\max} - \sigma_{\min})}{\left(\frac{\text{SL}_{\max} - \text{SL}_{\min}}{\text{SL}_{\min}}\right)}$$

where  $\text{SL}_{\min}$  and  $\text{SL}_{\max}$  represent the minimum and maximum limits of the linear region of the sarcomere length-stress relationship,  $\sigma_{\min}$  and  $\sigma_{\max}$  represent the calculated stresses at these respective sarcomere lengths,  $\Delta\sigma_f$  represents the change in fiber stress,  $\Delta\epsilon_f$  represents the change in fiber strain over this linear region, and  $E_f$  represents fiber elastic modulus. In contrast to the single-fiber data previously presented,<sup>5</sup> sarcomere length-stress relationships were all nonlinear. Thus, tangent modulus was measured over the linear portion of the curve so that tangent moduli reported were measured over a sarcomere length range of  $1.13 \pm 0.48 \mu\text{m}$  for normal bundles and  $1.44 \pm 0.78 \mu\text{m}$  for spastic bundles.

**Tissue Storage and Morphometry.** At the conclusion of the mechanical test, the bundle was pinned at rest length into a small plastic cassette (Tissue-Tek, Miles, Inc., Elkhart, IN) filled with embedding medium (Miles Laboratories, Naperville, IL). It was placed in a straight position in the middle of the mould to simplify transverse sectioning. The entire sample was frozen in liquid nitrogen-cooled isopentane ( $-159^\circ\text{C}$ ) and stored at  $-80^\circ\text{C}$  until analyzed.

Cross-sections (10  $\mu\text{m}$  thick) taken from the mid-portion of the tissue block were cut on a cryostat at  $-25^\circ\text{C}$  (Microm HM500, Walldorf, Germany). Serial sections were stained with hematoxylin-eosin to observe general tissue morphology, and labeled with primary antibodies to either the fast (NCL-MHCf, Novacastra, Newcastle, UK) or slow (NCL-MHCs, Novacastra, Newcastle, UK) myosin heavy chain (MHC). The secondary antibody used for visualization was biotinylated goat anti-mouse immunoglobulin G (Zymed Laboratories, San Francisco, CA). Immunoreactivity was visualized by StreptABCComplex (Dako, Glostrup, Denmark) using 3,3'-diaminobenzidine (DAB; Sigma-Aldrich, Steinheim, Germany) as the chromagen.

Muscle fiber size within each bundle was quantified by manually tracing the outline of each cell within the best tissue section (ImageJ, a public domain image analysis program freely available at <http://rsb.info.nih.gov/ij/index.html>). Interobserver error between two observers was 8.5%, and intraobserver error for repeated analysis of the same section by a single observer was 7.3%. Sections were characterized by an easily identifiable intermyofibrillar network, tight fiber packing, and polygonally shaped fibers. However, based on the fragility and small size of these bundles, numerous fixation and sectioning artifacts were noted, especially in the samples obtained from spastic muscles. The primary artifacts observed included oblique sectioning

**Table 1.** Muscle fiber bundle properties.

Parameter measured	Normal ( <i>n</i> = 21)	Spastic ( <i>n</i> = 9)
Fiber bundle length (mm)	2.78 ± 0.19	1.90 ± 0.24*
Number of fibers	18.1 ± 1.55	13.0 ± 1.45
Fast MHC (%)	50.6 ± 3.9	58.4 ± 8.1
Slow MHC (%)	39.4 ± 4.7	32.4 ± 8.3
Coexpressed MHC (%)	9.6 ± 3.6	9.2 ± 3.6
Ultimate stress (MPa)	150.4 ± 25.7	50.3 ± 11.7*
Peak sarcomere length (μm)	4.02 ± 0.20	4.04 ± 0.39
Cross-sectional area (μm <sup>2</sup> )	94,801 ± 9688	87,725 ± 18,639

Data are presented as mean ± SEM. MHC, myosin heavy chain.

\*Significant difference between tissue types (*P* < 0.05).

of certain cells and exaggerated separation of fibers within the bundle. To avoid erroneous measurement of large oblique fibers, the very long, oblong-shaped fibers were excluded from analysis. In addition, it was not feasible to measure bundle area directly because fibers dissociated from one another, leaving the appearance of increased extracellular space. Using these exclusion criteria, 18 fibers from a total of 289 fibers in 30 bundles were eliminated from the analysis. Exclusion of such irregular fibers did not affect any of the statistical analyses performed.

**Data and Statistical Analysis.** Data were grouped by specimen type (fiber vs. bundle) and tissue type (normal vs. spastic) and analyzed by two-way analysis of variance (ANOVA). Data were screened for normality and skew to justify the use of parametric statistics.<sup>23,24</sup> Post hoc multiple *t*-tests were used to make specific comparisons between bundles and cells of a given type and between matching specimens of different types. Thus, the multiple *t*-tests were corrected for these four comparisons, which were chosen a priori. Data are presented as mean ± SEM unless otherwise noted. Mathematical partitioning of tangent modulus and ultimate tensile stress was based on the assumption that muscle cells and the ECM acted mechanically in parallel. Bundle area vs. sarcomere length data were fit to a second-order polynomial and coefficients of determination used to determine fit quality.

## RESULTS

**General Bundle Characteristics.** Overall, bundles obtained from spastic muscles were inferior in quality compared to normal muscle. For example, spastic bundles were more mechanically fragile and thus the length of the spastic bundles tested was significantly shorter than the length of normal bundles (*P* < 0.05; Table 1). Additionally, diffraction patterns from spastic bundles were more diffuse and of a lower

intensity compared to those obtained from normal muscle, although sarcomere lengths were easily calculated. Finally, spastic bundles were characterized by a relatively large amount of extracellular flocculent material, which obscured transillumination by coherent laser or broadband white light. Bundles from both spastic and normal muscle were of the same cross-sectional area and had similar myosin heavy chain distributions, and contained a similar number of muscle fibers (*P* > 0.05; Table 1).

Increased extracellular material was easily observed by light microscopy in spastic samples (Fig. 2); this material was not simply an artifact of preparation as was observed with some normal samples (e.g., Fig. 3A). Whereas muscle cells from normal tissue generally retained a relatively polygonal shape (Fig. 3), spastic muscle fibers had a much more rounded, irregular appearance (Fig. 2). Approximately 50% of both normal and spastic muscle cells expressed only the fast MHC, ~40% expressed only the slow MHC, and a small fraction coexpressed both fast and slow MHC (Table 1).

**Bundle Mechanical Properties.** In contrast to mechanical results obtained from single cells of normal muscle in which the sarcomere length–stress rela-

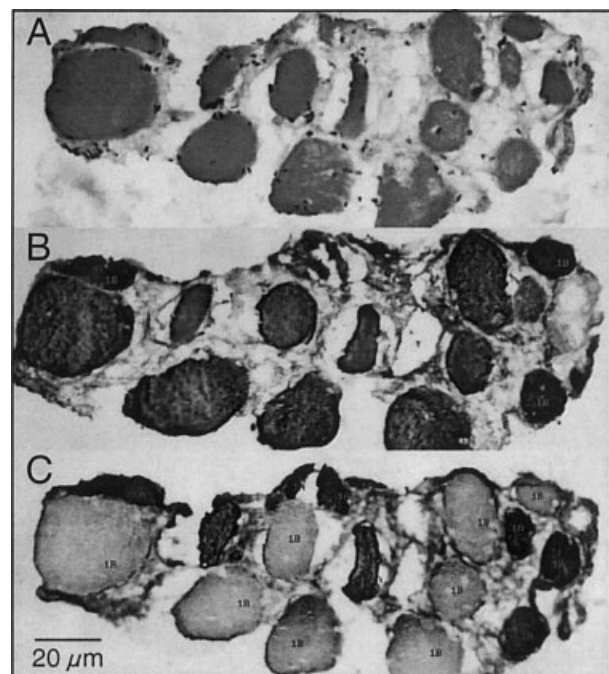


**FIGURE 2.** Light micrographs of serial sections of spastic muscle bundles after testing. (A) Hematoxylin–eosin staining for general morphology. (B) Immunohistochemical sectioned labeled with a primary antibody to the fast myosin heavy chain. (C) Immunohistochemical sectioned labeled with a primary antibody to the slow myosin heavy chain.

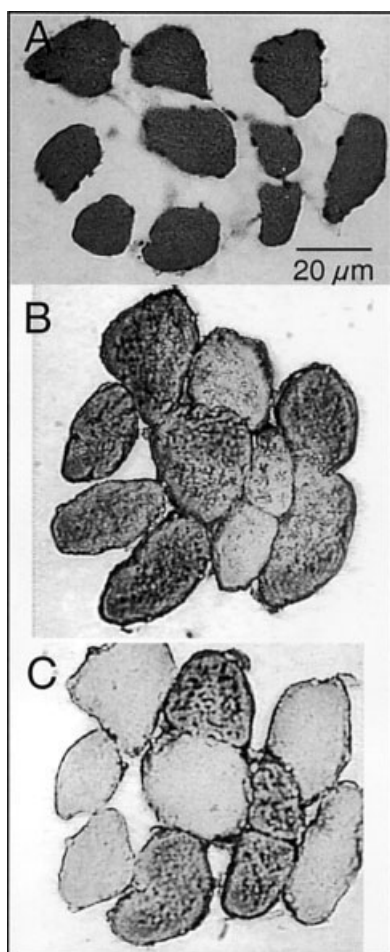


**FIGURE 3.** Light micrograph serial sections of normal muscle bundles after testing. **(A)** Hematoxylin–eosin staining for general morphology. **(B)** Immunohistochemical sectioned labeled with a primary antibody to the fast myosin heavy chain. **(C)** Immunohistochemical sectioned labeled with a primary antibody to the slow myosin heavy chain.

tionships were predominantly linear (e.g., as shown in Fig. 2A of Fridén and Lieber<sup>5</sup>), all sarcomere length–stress records from fiber bundles were nonlinear (Fig. 4). This suggests that the exponential shape observed was due to either interaction among fibers or to the added presence of the ECM. Since all curves were nonlinear, all moduli were expressed as a tangent modulus. Necessarily, the average sarcomere length range over which bundle tangent modulus is reported in the current study ( $1.22 \pm 0.11 \mu\text{m}$ , representing an average minimum sarcomere length of  $2.79 \pm 0.13 \mu\text{m}$  to an average maximum sarcomere length of  $4.02 \pm 0.18 \mu\text{m}$ ) was significantly shorter ( $P < 0.0001$ ) compared to the range previously reported for the modulus of single cells wherein linear stress–strain curves were usually observed ( $2.27 \pm 0.19 \mu\text{m}$ ).<sup>5</sup>

Slack sarcomere length was significantly shorter in fiber bundles of normal muscle compared to single cells, whereas slack sarcomere length was significantly longer in fiber bundles of spastic muscle compared to single cells using a simple *t*-test ( $P < 0.001$ ; Fig. 5A). Two-way ANOVA revealed a significant difference between spastic and normal tissue types ( $P < 0.005$ ) and a significant tissue-type  $\times$  specimen-type interaction ( $P < 0.0005$ ) for slack sarcomere length.

For both normal and spastic muscle, tangent modulus was significantly greater in bundles compared to single fibers ( $P < 0.0001$ ; Fig. 5B), but the difference was more pronounced for normal muscle than spastic muscle. In fact, whereas spastic muscle bundle modulus was only twice the single-fiber modulus, normal muscle bundle modulus was over 16 times greater than the modulus of a normal single muscle cell (Fig. 5B). Two-way ANOVA of tangent modulus revealed a significant effect of tissue type ( $P < 0.01$ ), a significant effect of specimen type ( $P < 0.0001$ ), and a highly significant interaction term ( $P < 0.005$ ). These data clearly suggest a dramatic difference in the behavior of spastic muscle bundles compared to normal muscle fiber bundles.

Consistent with our previous report, spastic muscle fibers were only one-third the size of normal fibers (Fig. 6A). However, since the spastic and normal bundles were approximately the same size (Table 1), only about 40% of the spastic bundle was occupied by muscle fibers, whereas 95% of the normal bundle was occupied by muscle (Fig. 6B).

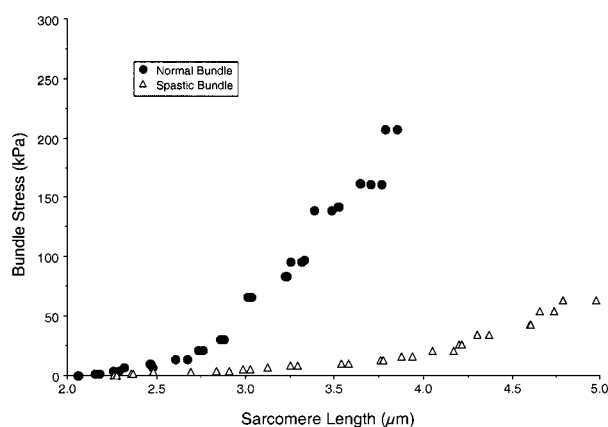


**FIGURE 4.** Examples of sarcomere length–stress curves measured from small muscle bundles. Normal sample obtained from the adductor pollicis muscle in a 45-year-old patient during fracture repair (filled circles) compared with a sample obtained from a spastic pronator teres muscle in an 11-year-old girl with static perinatal encephalopathy during tendon transfer surgery (open triangles).

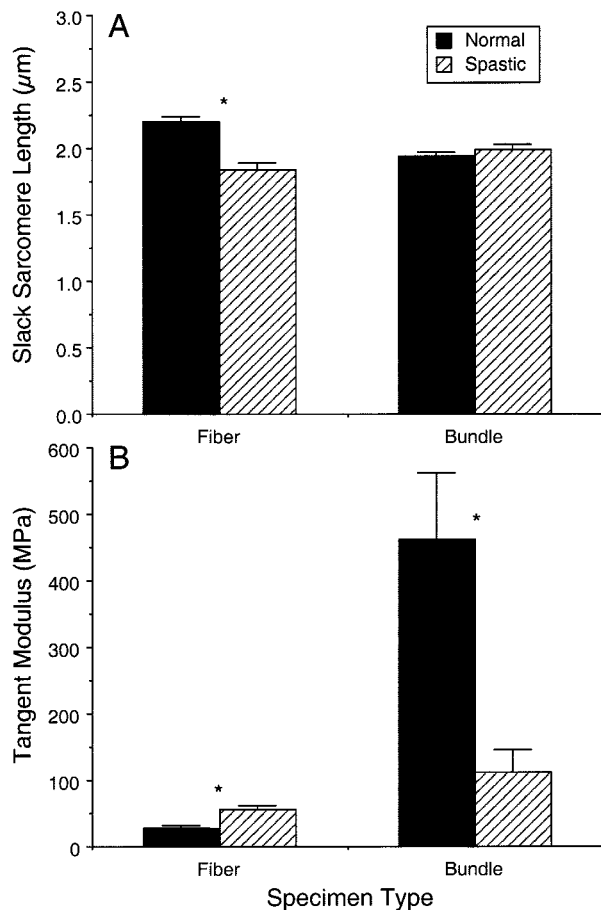


**FIGURE 5.** Biomechanical properties measured from single cells (left panels) and muscle fiber bundles (right panels) of normal (filled bars) and spastic (hatched bars) subjects. **(A)** Slack sarcomere length measured prior to mechanical testing. Two-way ANOVA revealed a significant difference between tissue types ( $P < 0.005$ ) and a significant tissue-type  $\times$  specimen-type interaction ( $P < 0.0005$ ) for slack sarcomere length. **(B)** Tangent modulus calculated from the linear portion of the sarcomere length–stress relationship. Two-way ANOVA of tangent modulus revealed a significant effect of tissue type ( $P < 0.01$ ), a significant effect of specimen type ( $P < 0.0001$ ), and a highly significant interaction term ( $P < 0.005$ ). Asterisks indicate  $P < 0.05$  by multiple  $t$ -test between normal and spastic specimens.

Further evidence of the decreased influence of muscle cells on the mechanical behavior of spastic bundles was obtained by plotting the change in bundle cross-sectional area as a function of sarcomere length during testing (Fig. 7). The normal relationship between fiber area and sarcomere length is well-approximated by a second-order polynomial since muscle volume remains constant during length change.<sup>1,7,16</sup> The average coefficient of determination of the normal data (Fig. 7A;  $0.92 \pm 0.06$ ) was greater than that calculated for the spastic data (Fig. 7B;  $0.83 \pm 0.20$ ), although the high variability in the

spastic group precluded achieving statistical significance. Qualitatively, the second-order relationship of normal muscle was more consistent compared to the relationship observed for spastic muscle.

## DISCUSSION

The purpose of this study was to determine the mechanical properties of fiber bundles obtained from both spastic and normal muscles. We had previously demonstrated that spastic muscle cells were stiffer and had a shorter resting sarcomere length than normal cells.<sup>5</sup> The most likely explanation for this observation was a modification of the intramuscular protein titin, which has been shown to bear the majority of the resting tension in skeletal muscle.<sup>10,15</sup> However, in contrast to detailed studies in frog muscle<sup>16</sup> demonstrating that the effect of intracellular

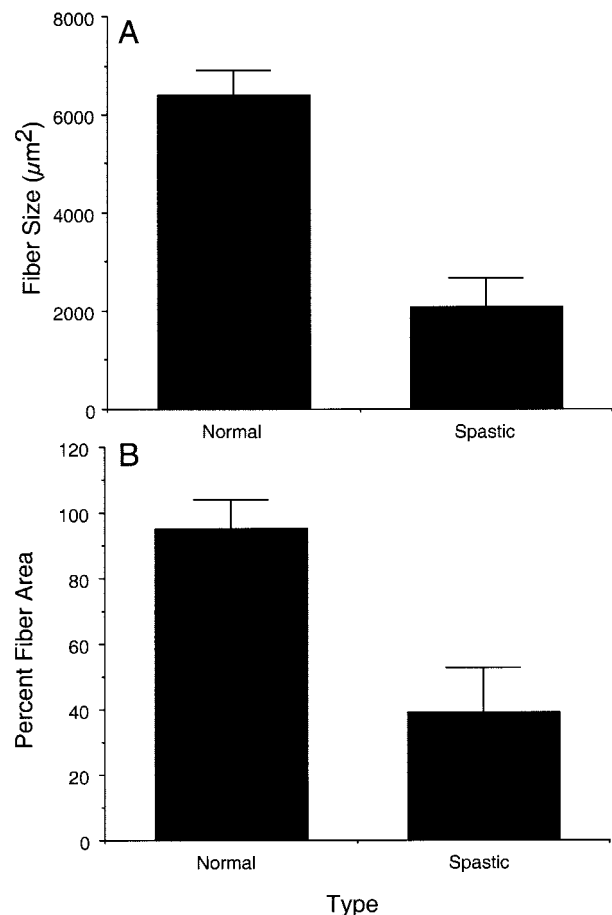


**FIGURE 6.** Morphological properties measured from muscle bundles of normal and spastic subjects. **(A)** Muscle fiber area digitized from light micrograph cross-sections. **(B)** Percentage of bundle cross-sectional area occupied by muscle fibers. Note that a much larger proportion of spastic muscle bundles is occupied by extracellular material.

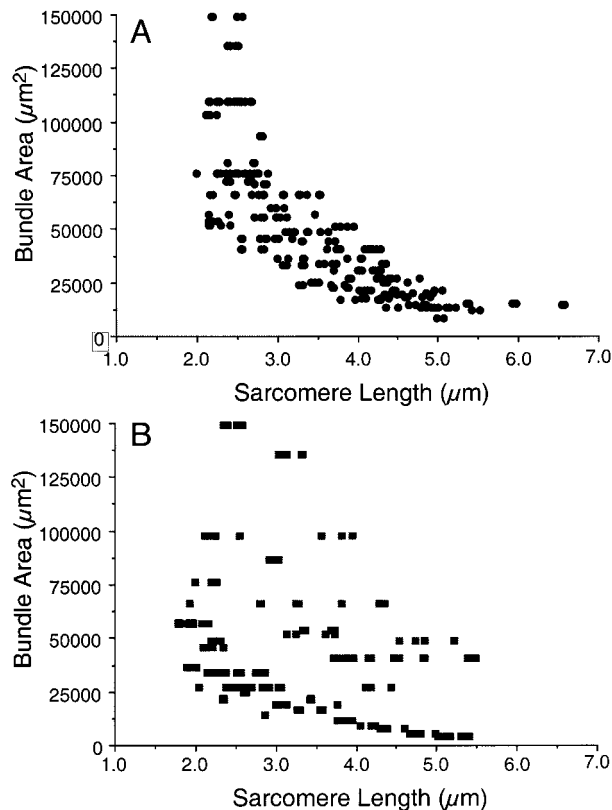


**FIGURE 7.** Relationship between sarcomere length and bundle cross-sectional area during elongation. **(A)** Normal muscle. **(B)** Spastic muscle. Note that the normal muscle behavior is much more isovolumic compared to spastic muscle. This may reflect the larger area fraction of muscle cells within normal muscle compared to spastic muscle.

proteins (presumably titin) dominated the passive mechanical properties even of whole muscle, a far more significant mechanical role for the ECM was revealed in the human muscle samples examined herein.

The most significant mechanical difference between normal and spastic muscle was the higher tangent modulus of small bundles compared to single cells (Fig. 5B). In normal muscle, the addition of the ECM dramatically increased the modulus from  $\sim 28$  kPa to  $\sim 470$  kPa, a 16-fold increase (filled bars in Fig. 5B). This is especially impressive in light of the calculation in the current study that the ECM of normal muscle made up only 5% of the specimen cross-section (Fig. 6B). This estimate is consistent with other morphometric estimates.<sup>4,12,26</sup> Considering the muscle and ECM to be acting in parallel, the tangent modulus of the normal ECM would be calculated to be  $\sim 8.5$  GPa, extremely stiff for mammalian connective tissue, which has been reported to have a modulus ranging from 1 to 3 GPa.<sup>8,14,18</sup> How-

ever, it should be noted that these previous reports are based on measurements made on isolated intact external tendons, which may not adequately represent either the structural or material properties of the complex intramuscular connective tissue milieu.<sup>25,26</sup> The values reported herein represent the first estimates of tensile modulus for the intramuscular connective tissue matrix based on direct mechanical measurements. The idea that this matrix may exceed the modulus of the external tendon is not surprising based on the relatively rough estimate of the true load-bearing area of the connective tissue matrix. Future studies are required to refine these estimates.

Surprisingly, spastic muscle bundles had a modulus that was only twice the fiber modulus (hatched bars in Fig. 5B). Apparently, this was due to the relatively small area fraction of stiff muscle cells (Fig. 5B) embedded in a large quantity of low-quality ECM (Fig. 6B). Again, considering the muscle and ECM to be acting in parallel, the tangent modulus of the spastic ECM would be calculated to be only  $\sim 0.20$  GPa, 45 times lower than that calculated for normal ECM and much lower than any literature value reported for connective tissue. The structural basis for the inferior mechanical properties of the spastic ECM is not known. Morphologically, the spastic ECM appeared disorganized, “loose” (not dense), and hypercellular (e.g., Fig. 2). This may represent a dynamic reorganization of the spastic ECM in response to altered muscle fiber mechanical properties, or the altered muscle fiber mechanical properties may be an attempt by the muscle cells to compensate for the deranged ECM. It is also possible that the inferior quality of the ECM may, in part, be responsible for the surprisingly highly elongated sarcomeres in wrist flexors after contracture, which were recently measured *in vivo*.<sup>11</sup> Based on measurements of hydroxyproline content, Booth et al. demonstrated that clinical measures of spasticity severity correlated significantly with collagen content.<sup>2</sup> Although these investigators did not specifically address the quality of the connective tissue, they concluded that the increased amount of collagen I in spastic muscle suggests that thickening of endomysium plays a role in the change of stiffness. The possibility also exists that some of the differences observed between tissue types is a reflection of the large age differences between specimens based on the report of increasing endomysial connective tissue with age.<sup>9</sup> However, the extent to which age affects the properties reported here is not yet known.

These findings have significant implications for the surgeon involved with reconstructive surgery of

both normal and spastic patients. The data indicate that, in normal muscle tissue, the ECM dominates the “feel” of the whole muscle since its tensile modulus is over 300 times that of the muscle cells. Therefore, even though a small amount of ECM is present in normal muscle, its functional impact is profound. This means that, when a surgeon pulls on a muscle to “tension” it during tendon transfer,<sup>22</sup> the sense of resistance is probably dominated by the ECM rather than the muscle cells themselves. This is not the case for spastic muscle in spite of the large amount of ECM. The spastic ECM has a modulus that is only four times greater than its fibers and, since the bundle is approximately 60% ECM and 40% fibers (Fig. 6B), the “feel” of a spastic muscle represents much more of a balance between ECM and fibers compared to normal muscle. Thus, during surgical manipulation of spastic muscle, the “feel” of the tissue is more closely related to the properties of the muscle fibers themselves. Further studies are required to provide surgeons with specific guidelines for specific muscles in order to determine the precise extent to which each muscle should be elongated during surgical manipulation.

This work was supported by NIH grants AR40050, AR40539, and HD044822, the United States Department of Veterans Affairs, and a Swedish Research Grant (11200).

## REFERENCES

- Baskin RJ, Paolini PJ. Volume change and pressure development in muscle during contraction. *Am J Physiol* 1967;213:1025–1030.
- Booth CM, Cortina-Borja MJ, Theologis TN. Collagen accumulation in muscles of children with cerebral palsy and correlation with severity of spasticity. *Dev Med Child Neurol* 2001;43:314–320.
- Dimitrijevic MR. Spasticity. In: Swash M, Kennard C, editors. *Scientific basis of clinical neurology*. New York: Churchill Livingstone; 1985. p 108–115.
- Eisenberg BR. Quantitative ultrastructure of mammalian skeletal muscle. In: Peachey LD, Adrian RH, Geiger SR, editors. *Skeletal muscle*. Vol. 10. Baltimore, MD: American Physiological Society; 1983. p 73–112.
- Fridén J, Lieber RL. Spastic muscle cells are shorter and stiffer than normal cells. *Muscle Nerve* 2003;27:157–164.
- Fung YC. *Biomechanics: mechanical properties of living tissues*. New York: Springer; 1981. 433 p.
- Haselgrove JC. Structure of vertebrate striated muscle as determined by x-ray-diffraction studies. In: *Handbook of physiology*. Bethesda, MD: American Physiological Society; 1983. p 143–171.
- Ker RF, Alexander RM, Bennett MB. Why are mammalian tendons so thick? *J Zool* 1988;216:309–324.
- Kovanen V, Suominen H, Peltonen L. Effects of aging and life-long physical training on collagen in slow and fast skeletal muscle in rats. A morphometric and immuno-histochemical study. *Cell Tissue Res* 1987;248:247–255.
- Labeit S, Kolmerer B. Titins: giant proteins in charge of muscle ultrastructure and elasticity. *Science* 1995;270:293–296.
- Lieber RL, Fridén J. Spasticity causes a fundamental rearrangement of muscle–joint interaction. *Muscle Nerve* 2002; 25:265–270.
- Lieber RL, Fridén JO, Hargens AR, Feringa ER. Long-term effects of spinal cord transection of fast and slow rat skeletal muscle. II. Morphometric properties. *Exp Neurol* 1986;91: 435–448.
- Linke WA, Stockmeier MR, Ivemeyer M, Hosser H, Mundel P. Characterizing titin’s I-band Ig domain region as an entropic spring. *J Cell Sci* 1998;111:1567–1574.
- Loren GJ, Lieber RL. Tendon biomechanical properties enhance human wrist muscle specialization. *J Biomech* 1995;28: 791–799.
- Magid A, Law DJ. Myofibrils bear most of the resting tension in frog skeletal muscle. *Science* 1985;230:1280–1282.
- Magid A, Reedy MK. X-ray diffraction observations of chemically skinned frog skeletal muscle processed by an improved method. *Biophys J* 1980;30:27–40.
- Mirbagheri MM, Barbeau H, Ladouceur M, Kearney RE. Intrinsic and reflex stiffness in normal and spastic, spinal cord injured subjects. *Exp Brain Res* 2001;141:446–459.
- Proske U, Morgan DL. Stiffness of cat soleus muscle and tendon during activation of part of muscle. *J Neurophysiol* 1984;52:459–468.
- Rose J, Haskell WL, Gamble JG, Hamilton RL, Brown DA, Rinsky L. Muscle pathology and clinical measures of disability in children with cerebral palsy. *J Orthop Res* 1994;12:758–768.
- Sinkjaer T, Magnussen I. Passive, intrinsic and reflex-mediated stiffness in the ankle extensors of hemiparetic patients. *Brain* 1994;117:355–363.
- Sinkjaer T, Toft E, Larsen K, Andreassen S, Hansen HJ. Non-reflex and reflex mediated ankle joint stiffness in multiple sclerosis patients with spasticity. *Muscle Nerve* 1993;16: 69–76.
- Smith RJ, Hastings H. Principles of tendon transfers to the hand. *AAOS Instruct Course Lect* 1993;21:129–149.
- Sokal RR, Braumann CA. Significance tests for coefficients of variation and variability profiles. *Syst Zool* 1980;29:50–66.
- Sokal RR, Rohlf FJ. *Biometry*. San Francisco: Freeman; 1981. 653 p.
- Trotter JA. Interfiber tension transmission in series-fibered muscles of the cat hindlimb. *J Morphol* 1990;206:351–361.
- Trotter JA, Purslow PP. Functional morphology of the endomysium in series fibered muscles. *J Morphol* 1992;212:109–122.
- Wood DJ, Zollman J, Reuban JP, Brandt PW. Human skeletal muscle: properties of the ‘chemically skinned’ fiber. *Science* 1975;187:1075–1076.
- Xu H, Christmas P, Wu XR, Wewer UM, Engvall E. Defective muscle basement membrane and lack of M-laminin in the dystrophic dy/dy mouse. *Proc Natl Acad Sci USA* 1994;91: 5572–5576.